HHS Public Access

Author manuscript

Mol Cancer Res. Author manuscript; available in PMC 2018 December 17.

Published in final edited form as:

Mol Cancer Res. 2017 June ; 15(6): 660–669. doi:10.1158/1541-7786.MCR-17-0028.

CDK4/6 Therapeutic Intervention and Viable Alternative to Taxanes in CRPC

James P. Stice[1], **Suzanne E. Wardell**[1], **John D. Norris**[1], **Alexander P. Yllanes**[1], **Holly M. Alley**[1], **Victoria O. Haney**[1], **Hannah S. White**[2], **Rachid Safi**[1], **Peter S. Winter**[1], **Kimberly J. Cocce**[1], **Rigel J. Kishton**[1], **Scott A. Lawrence**[1], **Jay C. Strum**[2], and **Donald P. McDonnell**[1]

[1]Department of Pharmacology and Cancer Biology, Duke University School of Medicine, Durham, North Carolina.

[2]G1 Therapeutics, Inc., Research Triangle Park, North Carolina.

Abstract

Resistance to second-generation androgen receptor (AR) antagonists and CYP17 inhibitors in patients with castration-resistant prostate cancer (CRPC) develops rapidly through reactivation of the androgen signaling axis and has been attributed to AR overexpression, production of constitutively active AR splice variants, or the selection for AR mutants with altered ligand-binding specificity. It has been established that androgens induce cell-cycle progression, in part, through upregulation of cyclin D1 (CCND1) expression and subsequent activation of cyclin-dependent kinases 4 and 6 (CDK4/6). Thus, the efficacy of the newly described CDK4/6 inhibitors (G1T28 and G1T38), docetaxel and enzalutamide, was evaluated as single agents in clinically relevant *in vitro* and *in vivo* models of hormone-sensitive and treatment-resistant prostate cancer. CDK4/6 inhibition (CDK4/6i) was as effective as docetaxel in animal models of treatment-resistant CRPC but exhibited significantly less toxicity. The *in vivo* effects were durable and importantly were observed in prostate cancer cells expressing wild-type AR, AR mutants, and those that have lost AR expression. CDK4/6i was also effective in prostate tumor models expressing the AR-V7 variant or the AR F876L mutation, both of which are associated with

Corresponding Author: Donald P. McDonnell, Duke University School of Medicine, LSRC BLDGRMC238, Box 3813 DUMC, Durham, NC 27710. Phone: 919-684-6035; Fax: 191-9681-7139; donald.mcdonnell@duke.edu.

Authors' Contributions

Conception and design: J.P. Stice, S.E. Wardell, D.P. McDonnell

Development of methodology: J.P. Stice, S.E. Wardell

Acquisition of data (provided animals, acquired and managed patients, provided facilities, etc.): J.P. Stice, S.E. Wardell, J.D. Norris, A.P. Yllanes, H.M. Alley, V.O. Haney, H.S. White, R. Safi, P.S. Winter, K.J. Cocce, R.J. Kishton, S.A. Lawrence

Analysis and interpretation of data (e.g., statistical analysis, biostatistics, computational analysis): J.P. Stice, S.E. Wardell, H.S. White, R. Safi, P.S. Winter, D.P. McDonnell

Writing, review, and/or revision ofthe manuscript: J.P. Stice, S.E. Wardell, J.C. Strum, D.P. McDonnell

Administrative, technical, or material support (i.e., reporting or organizing data, constructing databases): J.P. Stice, S.E. Wardell, H.M. Alley, J.C. Strum, D.P. McDonnell

Study supervision: S.E. Wardell, D.P. McDonnell

Other (inventor of G1T28 and G1T38 used in this article): J.C. Strum

Disclosure of Potential Conflicts of Interest

H.S. White and J.C. Strum are compensated employees of G1 Therapeutics. J.P. Stice has previously served as a compensated consultant for G1 Therapeutics. D.P. McDonnell is a member of the SAB (compensated) for G1 therapeutics and holds equity in the company. No potential conflicts of interest were disclosed by the other authors.

Note: Supplementary data for this article are available at Molecular Cancer Research Online (http://mcr.aacrjournals.org/). J.P. Stice and S.E. Wardell contributed equally to this article.

treatment resistance. Furthermore, CDK4/6i was effective in prostate cancer models where AR expression was lost. It is concluded that CDK4/6 inhibitors are a viable alternative to taxanes as therapeutic interventions in endocrine therapy–refractory CRPC.

Introduction

Prostate cancer is the second leading cause of cancer-related deaths and the most commonly diagnosed cancer in men in the United States (1). In this cancer, the androgen receptor (AR) is a key oncogenic driver responsible for the regulation of genes whose products are required for cell growth, survival, and metastasis (2). Not surprisingly, therefore, disruption of the AR signaling axis by inhibiting testicular androgen production using luteinizing hormone–releasing hormone agonists (or antagonists) or direct inhibition of AR signaling using antiandrogens remain first-line therapeutic options for patients diagnosed with prostate cancer (3). Although these treatments prolong overall survival of prostate cancer patients, resistance eventually emerges in the majority of patients by mechanisms that remain dependent on AR signaling (4). Indeed, it is now well established that relapse is associated with the reactivation of the androgen signaling axis through increased intratumoral androgen production, AR overexpression, production of constitutively active AR splice variants (AR-V1 or AR-V7), or the outgrowth of cells that express gain-of-function mutations in the AR ligand–binding domain that enable some antiandrogens to be recognized as agonists (5–11). Some tumors in which these resistance mechanisms manifest can be treated with third-generation AR antagonists, such as enzalutamide, or with the CYP17 inhibitor abiraterone, a drug that decreases adrenal and intratumoral production of androgens. However, the duration of response to even the most contemporary inhibitors of AR signaling is relatively short, and the therapeutic options for patients progressing while on these drugs are generally limited to taxanes (12–14). It has recently been reported that progression during abiraterone or enzalutamide treatment is associated with the appearance of the constitutively active AR-V7 variant. This is particularly problematic as all of the currently available AR-directed therapies target the ligand-binding domain of the receptor, a domain not present in AR-V7. This observation, together with the identification of mutations in AR that enable enzalutamide to manifest agonist activity in tumors of treated patients, highlight the difficulty of further targeting this receptor using established approaches. Thus, there is an unmet medical need for therapeutics that target pathways downstream of AR that are required for tumor pathogenesis.

AR (and AR variants) drives cell-cycle progression in part through the upregulation of cyclin D1 expression and the subsequent activation of the G_1 cyclin-dependent kinases (CDK4/6; ref. 15). Although not studied extensively in prostate cancer, the CDK4/6 inhibitors palbociclib, ribociclib, and abemaciclib have all demonstrated efficacy when evaluated as single agents or in combination with antihormonal therapy, chemotherapy, or radiation in retinoblastoma-positive preclinical models of breast cancer (16, 17). Clinical trials have also demonstrated that palbociclib, in combination with aromatase inhibitors or antiestrogens, is effective in advanced estrogen receptor–positive (ER^+) breast cancer tumors that have progressed while on endocrine therapy (18, 19). It is surprising, considering the similar roles of the cyclin D1–CDK4/6 axis in prostate and breast cancers, that CDK4/6 inhibitors have

not been assessed for clinical utility in patients with castration-resistant prostate cancer (CRPC). Consideration of this treatment modality in prostate cancer may have been delayed by the significant toxicity of the first-generation CDK4/6 inhibitors and the relatively recent appreciation of the extent of, and mechanisms underlying, the development of resistance to less toxic interventions, such as enzalutamide and abiraterone.

The clinical experience with the first-generation, broad-spectrum CDK inhibitors was disappointing with regard to both efficacy and their significant toxicity (reviewed in ref. 20). However, recent experience with more selective CDK4/6 inhibitors has been much more positive, and drugs of this class are likely to become a cornerstone in treatment regimens for luminal breast cancer and other cancers. Notwithstanding this success, the myelosuppression associated with the continuous administration of existing CDK4/6 inhibitors limits their more widespread use in cancer therapies. Whereas the neutropenia and leukopenia associated with palbociclib and ribociclib administration can be partially resolved with regular (every 4th week) withdrawal of the inhibitor, there is concern that these “treatment vacations” may actually contribute to the development of resistance (21, 22). Abemaciclib, on the other hand, can be dosed continuously without negatively impacting the bone marrow, although its intrinsic side effect profile is also an impediment to its more widespread use (23). With the assumption that some of the side effects of the existing inhibitors can be attributed to their off-target activities, efforts were made to identify a new series of highly selective CDK4/6 inhibitors, a discovery campaign that led to the development of G1T28 and G1T38. These compounds, which are currently under clinical development, are highly selective for their targets and were shown to induce significantly less myelosuppression than palbociclib in several animal models (24, 25). Thus, in this study, we have examined the activity of G1T28 and G1T38 in preclinical models of CRPC as a prelude to their evaluation in clinical trials for the treatment of CRPC.

Materials and Methods

Cell lines and reagents

Reagents were obtained from the following sources: R1881, PerkinElmer; MDV3100, palbociclib, abiraterone acetate, docetaxel (*in vitro*), Selleckchem; and docetaxel (*in vivo*), Duke University Hospital (Durham, NC). G1T28: [2′-((5-(4-methyl-piperazin-1-yl)pyridin-2-yl)amino)-7′,8′-dihydro-6′ H-spiro [cyclohexane-1,9′pyrazino[1′,2′:1,5]pyrrolo[2,3-d]pyrimidin]-6′-one] and G1T38: 2′-((5-(4-isopropylpiperazin-1-yl)pyridin-2-yl)amino)-7′,8′ dihydro-6′H-spiro[cyclohexane1,9′pyrazino [1′,2′:1,5]pyrrolo[2,3-d]pyrimidin]-6′-one were provided by G1 Therapeutics, Inc. All cell lines used were obtained from ATCC, which employs STR verification. Cells were not maintained in culture longer than 4 months.

In-cell Western assay

22rV1 cells or VCaPs were plated in RPMI or DMEM supplemented with 8% FBS in 96-well clear-bottom black plates (1.5×10^4 or 2.5×10^4 cells/well). After 48 hours, cells were treated with G1T28 or G1T38 for 24 hours. Cells were fixed with formalin, permeabilized using PBS (0.1% Triton X-100), and incubated with phospho retinoblastoma T807/811

(D20B12, Cell Signaling Technology, 1:2,000), total retinoblastoma (4H1, Cell Signaling Technology, 1:1,000), anti-AR antibody (N-20, Santa Cruz Bio-technology, 1:2000), or actin (A5316, Sigma, 1:10,000) overnight. Cells were washed with PBS (0.1% Tween), and stained with second antibody (Biotium CF680 goat anti-mouse or CF770 goat anti-rabbit at 1:2,000). Protein expression was assessed using the LI-COR Odyssey imaging system.

Cell proliferation assay

LNCaP, LnCaP-XIP, LNCaP-AR, LNCaP-F876L (5×10^3 cells/well), VCaP (1×10^4 cells/well), PC-3, DU145, and 22Rv1 (4×10^3 cells/well) were plated in 96-well tissue culture plates, and after 24 hours were treated as indicated and incubated for 5 to 7 days. Cellular proliferation was assessed by Hoechst staining of DNA content.

Cell-cycle analysis

Cells were seeded in media containing 8% FBS between 1.2×10^5 and 3×10^5 cells per well in 12-well plates and allowed to grow for 48 hours before addition of the indicated treatments in duplicate. Cells were harvested and fixed in 70% (v/v) cold ethanol at −20° C overnight. After washing (PBS), fixed cells were collected (centrifugation) and resuspended in PI/RNase (Sigma) for DNA staining and analysis (BD Accuri C6 flow cytometer). Data were analyzed using the CFlow Plus program software (BD Biosciences).

Apoptosis assay

VCaP (3×10^5 cells/well) and 22Rv1 (1.2×10^5 cells/well) were plated in DMEM containing 8% FBS and the indicated compound for 24 to 72 hours. Cells were trypsinized, washed, and double stained with Alexa Fluor 488 Annexin V and Sytox Red (Invitrogen) according to the manufacturer's instructions. Percentage of apoptotic (Annexin V positive) cells within the total number of cells was calculated. A total of 10,000 events were collected for each sample (BD Accuri C6 flow cytometer) and data were analyzed using the CFlow Plus program software (BD Biosciences).

Neutrophil isolation

Bone marrow were flushed from tibia and femur bones of mice, strained (0.22 μmol/L cell filter), and resuspended in PBS containing 1% BSA and 10% FBS. Total cell number was quantified and an aliquot was stained using FITC-CD11b (M1/70, BD Biosciences) and APC-Ly-6G (RB6-8C5, Affymetrix). CD11b/Ly-6G$^+$ cells were quantified using a MACSQuant flow cytometer, and data were analyzed using the MACSQuantify program software (Miltenyi Biotec).

Animal studies

All procedures were approved by the Duke University Institutional Animal Care and Use Committee.

LNCaP-AR-F876L xenograft.—Male NSG (NOD.Cg-Prkdc^{scid} Il2rg^{tm1Wjl}/SzJ) mice (in-house colony) were castrated at 6 weeks of age, 10 days prior to injection of 3×10^6 LNCaP-ARF876L cells subcutaneously into the flank. Tumor growth was measured 3 times

weekly by caliper [tumorvolume = ($A^2 \times B$)/2, where A < B]. When tumor volume reached approximately 0.1 cm^3, mice were randomized (n = 12–14) to 56 days of daily oral gavage with vehicle (10 mmol/L citrate, pH 4), enzalutamide (30 mg/kg formulated in 1% carboxymethyl-cellulose/0.1% Tween 80), docetaxel (vehicle gavage daily and once weekly intraperitoneal injection with 20 mg/kg docetaxel diluted in sterile saline), or G1T38 (50 or 100 mg/kg formulated in vehicle).

22rV1 xenograft.—Six-week-old male NU/NU mice (in-house colony) were castrated 10 days prior to injection of 1×10^6 22rV1 cells subcutaneously and tumor measurement was performed as above.

Efficacy.—When tumor volume reached 0.13 to 0.22 cm^3, mice were randomized (n = 15 unless otherwise indicated) to treatment with vehicle, docetaxel, or G1T28 (100 mg/kg in citrate buffer vehicle), G1T38 (10, 50, or 100 mg/kg), formulated, and administered as above. On treatment day 14, vehicle (n = 31)-treated mice were rerandomized to treatment with vehicle (n = 15) or 100 mg/kg G1T38 (n = 16). On treatment day 31, animals receiving 100 mg/kg G1T38 (n = 34) with static tumor volume (≤2-fold change during treatment, n = 27) were rerandomized to an additional 23 days of treatment with vehicle (n = 13) or 100 mg/kg G1T38 (n = 14).

Pharmacokinetics.—Animals were randomized (n = 25) 12 days after tumor implant (average tumor volume = 0.19 cm^3 ± 0.05 SD) to daily treatment with vehicle, G1T28 (100 mg/kg), or G1T38 (10, 50, or 100 mg/kg) formulated as above. Animals were euthanized (n = 5) 1, 6, 12, 24, or 24 hours after the 9th treatment. Statistical analyses were performed using GraphPad Prism 6 and are described below.

Complete blood count analyses

Whole blood was collected into tubes containing K_2EDTA after the ninth dose of G1T28 or G1T38. A complete blood count (CBC) was collected using an Abaxis HM5 five-part differential hematology analyzer.

Pharmacokinetic analyses

Whole-blood and tumor samples were collected in tubes containing K_2EDTA from individual animals at 1, 6, 12, 24, and 48 hours after the ninth dose of either G1T28 or G1T38. Plasma was obtained by centrifugation, and tumors were homogenized using a Bead Ruptor homogenizer with 2.8-mm zirconium ceramic oxide beads after adding 3 mL of 50/50 methanol/water per gram of tissue. G1T28 and G1T38 were extracted from mouse plasma or tumor homogenate by protein precipitation with acetonitrile. Before the extraction, G1T28-D3: 2′-((5-(4-methylpiperazin-1-yl)pyridin-2-yl)amino)-7′,8′-dihydro-6′H-spiro [cyclohexane-1,9′-pyrazino[1′,2′:1,5]pyrrolo[2,3-d]pyrimidin]-6′-one di-hydrochloride was added as an internal standard. A portion of the organic layer was transferred to a new 96-well plate containing an acetonitrile/water solution. The samples were injected into an LC/MS-MS system using an Allure PFP Propyl column with a mobile phase containing acetonitrile, water, ammonium formate, and formic acid. Detection was

done using a Sciex API4000 mass spectrometer with a turbo ionspray ionization source and MRM mode.

Statistical analyses

For LNCaP-AR-F876L and 22rV1 efficacy xenograft studies, using the sample size and power function in JMP statistical software (SAS Institute, Inc), a group size of $n = 13$ per treatment arm was estimated to be required to reliably detect a statistically relevant ($P < 0.05$) 25% change with 80% confidence, given the anticipated 15% variability for the tumor models utilized ($\alpha = 0.05$, SD = 0.15, confidence of 0.8, s/delta of 0.25). This estimate is based on one-way ANOVA followed by the Student Newman Keul test and is in accordance with current literature in the field. Animals were randomized to treatment when tumor size measured 0.12 to 0.22 cm^3 volume. Animals were allocated to treatment such that the average initial tumor volume per group was 0.16 to 0.17 ± 0.01 cm^3 volume. Average tumor volume and SEM for each group over 31 to 56 days of dosing are presented. These data were subjected to exponential growth curve analysis constrained to share an initial value, and to two-way ANOVA analysis followed by Bonferroni multiple comparison test. Groups showed equivalent variance (10%–15% with normal distribution) throughout all time points, justifying the statistical analyses that were selected. Standard survival curve (Kaplan–Meier analysis) was also applied to xenograft studies, using 200% of initial as an endpoint.

Results

CDK4/6 inhibition as a strategy to treat CRPC

The mitogenic actions of estrogens and androgens can be attributed in part to their ability to induce the expression of cyclin D1, which together with its catalytic partner(s) CDK4/6 forms a complex that phosphorylates retinoblastoma, facilitating the release of the sequestered E2F1 transcription factor. This transcription factor subsequently induces the expression of genes the products of which enable cells to traverse the G_1–S cell-cycle checkpoint. Not surprisingly, through their ability to block retinoblastoma phosphorylation, small-molecule inhibitors of CDK4/6 effectively inhibit the growth of retinoblastoma-positive, ER^+, breast cancers, and one drug of this class, palbociclib, is already approved for the treatment of metastatic breast cancer when used in combination with the aromatase inhibitor letrozole or the antiestrogen fulvestrant. Given the similar roles of estrogens and androgens in driving cell proliferation, it is not surprising that palbociclib was also found to be an effective inhibitor of tumor cell proliferation in preclinical models of prostate cancer (26). Whereas the activity of palbociclib as a prostate cancer therapeutic remains to be determined, its established myelosuppressive activity is likely to be dose limiting, especially when combined with docetaxel, the current standard of care in the setting of advanced disease. Recently, we have reported the development and characterization of a new class of highly selective, tricyclic lactam CDK4/6 inhibitors that exhibit reduced myelosuppressive activity (24), and in this study, we have evaluated their antitumor activity in clinically relevant *in vitro* and *in vivo* models of advanced CRPC.

The antiproliferative activity of the CDK4/6 inhibitors, G1T28 and palbociclib (PD-0332991), was evaluated first in well-validated cellular models of prostate cancer, and

their efficacy was compared with enzalutamide and docetaxel. For these studies, the AR-dependent LnCAP and VCaP prostate cancer cell lines were used, as was the 22rV1 cell model, which in addition to wtAR expresses a constitutively active AR-V7 variant that likely contributes to endocrine therapy resistance and to the emergence of CRPC. The growth of LnCAP and VCaP cells was inhibited in a similar manner by all of the agents tested, with both G1T28 and palbociclib exhibiting the same efficacy albeit with subtle, nonsignificant differences in potency. G1T28, palbociclib, and docetaxel all inhibited the growth of 22rV1 cells, whereas, expectedly, enzalutamide was without effect (Fig. 1A). Considering that G1T28 performed similarly to palbociclib in these assays, it was brought forward for a more comprehensive evaluation of its activity with a view to assessing its potential utility as a prostate cancer therapeutic.

As expected for a drug of its class, cell-cycle analysis confirmed that the antiproliferative activity of G1T28 in all three cell lines tested could be attributed to an accumulation of cells arrested in the G_0–G_1 stage of the cell cycle (Fig. 1B). This activity correlated with decreased retinoblastoma phosphorylation in both the androgen-dependent (VCaP) and independent (22Rv1) cell models evaluated (Fig. 1). Notably, the IC_{50}s of G1T28 in growth, cell cycle, and CDK4/6 inhibition (CDK4/6i) assays were very similar in each of the cell lines examined. At doses that maximally inhibited cell proliferation and retinoblastoma phosphorylation, G1T28 had no effect on the expression of wtAR (VCaP) or AR-V7 (22Rv1) and did not significantly inhibit the expression of AR target genes (i.e., ORM1 or PSA) in either cell line (Supplementary Fig. S1A and S1B). No changes in the expression of D or E cyclins or CDK4 were noted, although, as expected, a considerable reduction in the expression of cyclin A (an E2F1 target gene) was observed (Supplementary Fig. S1C; ref. 27). The ability to inhibit proliferation, without affecting the expression of AR or its target genes, suggested that G1T28 may also inhibit the growth of AR-negative prostate cancer cells. In evaluating this possibility, it was noted that treatment with G1T28 inhibited the growth of PC3, but not DU145 cells. Whereas both lines are AR-negative, in PC3 cells, unlike DU145 cells, retinoblastoma is constitutively active. Similar responses were observed when cells were treated with palbociclib, and as expected, enzalutamide was without effect in either of the AR-negative cells examined (Supplementary Fig. S1D). When taken together, these data suggest that CDK4/6i may be a useful approach to treat retinoblastoma-positive AR-dependent and AR-independent prostate cancers and that both of the inhibitors evaluated (G1T28 and palbociclib) were similarly effective in these *in vitro* assays.

G1T28 inhibits the growth of 22Rv1-derived tumor xenografts

Despite the development of (i) potent and effective inhibitors of cyp17 that decrease the production of adrenal and intratumoral androgens and (ii) third-generation antiandrogens that interfere with multiple steps in AR action, the development of resistance and progression of CRPC is an impediment to durable clinical responses. Whereas the mechanisms underlying the development of resistance are complex, it has been attributed in a significant number of cases to the overexpression of AR and/or to the expression of the constitutively active AR-V7 variant. Recently, increased AR-V7 expression has been shown to be highly predictive of response to androgen deprivation therapy, and thus, there is considerable interest of late in developing strategies that will inhibit the growth of prostate

tumors expressing this variant (6). Considering the results of the *in vitro* studies (above), it was of interest to evaluate the impact of G1T28 on the growth of the AR-V7–expressing 22Rv1 cells when propagated as xenografts in mice. As shown in Fig. 2, G1T28 (100 mg/kg) significantly inhibited tumor growth as compared with vehicle and docetaxel (20 mg/kg). At the end of the study, it was demonstrated that G1T28 treatment quantitatively inhibited retinoblastoma phosphorylation, and although not observed in the studies performed *in vitro*, the drug treatment also decreased the expression of total retinoblastoma (Supplementary Fig. S2A). The mechanisms and consequences of the latter activity are currently under investigation. A slight decrease in ARwt expression, but not of AR-V7, was also noted, but the significance of this finding in endpoint tumors is unclear (Supplementary Fig. S2A). Regardless, these results suggest that CDK4/6 inhibitors may have utility as prostate cancer therapeutics having a particularly useful characteristic of being able to inhibit the growth of tumors expressing the AR-V7 variant. Thus, we further explored the potential clinical utility of this class of drug in additional models of CRPC.

CDK4/6 inhibition in multiple models of antiandrogen resistance

G1T28 is currently being evaluated in two separate phase II clinical trials in patients with small-cell lung carcinoma as an approach to suppress the proliferation of hematopoietic stem and progenitor cells during chemotherapy, an activity that is expected to preserve the immune and hematopoietic systems. Here, the drug is administered intravenously to allow precise control of bone marrow arrest and proliferation. Thus, nearterm use of this particular compound in prostate cancer could be contemplated, but this route of administration is not ideal for an antineoplastic therapy. However, having established the utility of G1T28 in relevant models of prostate cancer, we were encouraged to explore G1T38 (chemical structure in Supplementary Fig. S2B), a closely related homolog of G1T28, in models of CRPC. To this end, the activity of G1T38 was assessed in relevant cellular and animal models of prostate cancer. Importantly, a comprehensive *in vitro* analysis revealed no discernable differences between G1T28 and G1T38 with respect to their ability to inhibit retinoblastoma phosphorylation, induce G_0–G_1 arrest, or inhibit the proliferation of AR-positive prostate cancer cells. In addition, like G1T28, G1T38 also inhibited the proliferation of PC3 but not DU 145 cells (Supplementary Fig. S3A–S3C).

Considering the functional equivalence of G1T28 and G1T38 *in vitro*, we next evaluated the antitumor activity of the latter drug in the 22Rv1 model of CRPC as outlined in Fig. 3A. In this study, it was observed that G1T38 (50 and 100 mg/kg does) significantly inhibited tumor growth and increased tumor doubling time compared with the vehicle arm (Fig. 3B). Equivalent, near complete inhibition of tumor growth was noted in the 100 mg/kg G1T38 and docetaxel treatment groups. Because of animal weight loss, docetaxel treatment was limited to 4 cycles (28 days with animals euthanized on treatment day 31), whereas body weights of animals treated with 100 mg/kg G1T38 remained consistent throughout the study (Supplementary Fig. S3D). An additional substudy was performed in which the animals receiving G1T38 (100 mg/kg) for 31 days (see Fig. 3B) were rerandomized ($n = 13$) to an additional treatment with vehicle or 100 mg/kg G1T38. The data from the vehicle treatment group from Fig. 3B are also shown for comparative purposes. It was observed that tumor growth resumed upon drug withdrawal, confirming the requirement for the continued

presence of drug to maintain growth suppression. However, at later points in the study, the tumors in some of the treated animals began to grow and exhibit drug resistance (Fig. 3C).

The underlying mechanisms by which the resistance observed occurs are currently under investigation. To assess the ability of G1T38 to suppress the growth of established tumors, we rerandomized animals ($n = 14$) from the vehicle treatment group at day 14 (tumor size of ~0.5 cm^3) to receive vehicle alone or G1T38 (100 mg/kg). In this manner, it was determined that G1T38 significantly decreased tumor growth, but tumor regression was not observed (Fig. 3D).

In addition to the expression of AR splice variants, resistance to endocrine therapy has been associated with (i) overexpression of wtAR, which amplifies the residual partial agonist activity of antagonists and (ii) point mutations within the ligand-binding domain of the receptor that enable it to recognize antagonists as agonists. One of the most recently discovered mutants in AR, F876L, renders prostate cancer cells resistant to enzalutamide. Considering the clinical importance of these resistance mechanisms, we have engineered LNCaP cells, which express AR T877A endogenously, to overexpress wild-type AR (XIP-AR) or AR F876L (XIP-AR F876L; ref. 28). Notably, Casodex-driven growth of XIP-AR cells and enza-lutamide-driven growth of XIP-AR F876L cells were both sensitive to CDK4/6i (Supplementary Fig. S4). As a follow-up, we assessed the extent to which CDK4/6i would be an effective strategy to inhibit the growth of LNCaP-AR-F876L cell-derived xenografts. The results of this study, shown in Fig. 4, indicate that although enzalutamide was without effect, G1T38 (100 mg/kg) was as effective as docetaxel, with 50 mg/kg G1T38 exhibiting moderate efficacy (Fig. 4).

Evaluation of the pharmacokinetic/pharmacodynamic properties of G1T28 and G1T38

A comparative analysis of the relationship between tumor response and intratumoral exposure to both G1T28 and G1T38 was undertaken. For this pharmacokinetic/pharmacodynamic study, we utilized the 22Rv1 xenograft model and measured drug levels in plasma and tumors following administration of G1T38 and G1T28 as outlined in Fig. 5A. Significant inhibition of tumor growth was observed after 8 days of treatment with G1T28 (only 100 mg/kg evaluated) or G1T38 (50 or 100 mg/kg doses), with G1T38 exhibiting greater growth suppression than G1T28 at the 100 mg/kg dose (Fig. 5B). Plasma and tumor levels of both drugs at all doses were measured at 1, 6, 12, 24, and 48 hours after final administration (day 9). The major conclusions from this analysis were that (i) the plasma and intratumoral levels of G1T38 were proportional to dose; (ii) significant retention of drug in the tumors was observed as long as 2 days following final dose; and (iii) the intratumoral levels of G1T28 were significantly higher than those of G1T38 at all time points (Fig. 5C). The pharmacologic basis for these activities is under investigation.

Myelosuppression, in particular neutropenia, is a dose-limiting toxicity of existing CDK4/6 inhibitors and is likely to be a class effect of this type of drug. Thus, for both G1T28- and G1T38- treated animals, we (i) performed a CBC analysis of blood (one hour after final dose) and (ii) assessed bone marrow neutrophil counts in animals euthanized 24 or 48 hours after final treatment. The CBC analysis revealed that G1T38 and G1T28 at all doses tested significantly reduced the numbers of circulating lymphocytes, while a modest repression of

neutrophils was noted. No decrease in RBCs was observed (Fig. 5D). Similarly, a modest repression in the number of CD11b/Ly-6G$^+$ neutrophils cells isolated from bone marrow was observed, with G1T28 demonstrating the greatest reduction at 24 and 48 hours (Fig. 5E). Although G1T28 demonstrated the highest exposure in both the plasma and tumors when compared with an equivalent dose of G1T38, it was found that G1T38 exhibited greater efficacy with less myelosuppression observed in bone marrow. Thus, considering these favorable activities, its antitumor activities, and the ability to deliver the drug orally, we have initiated a clinical development program to assess the activity of this drug in patients with CRPC.

Discussion

Despite the success of CDK4/6 inhibitors in breast cancer and the similarity in the mechanisms by which AR and ER impact cell proliferation, only one study has addressed the effects of CDK4/6i in prostate cancer. In that study, it was noted that palbociclib effectively inhibited LNCaP and VCaP cell proliferation, an activity that was dependent on retinoblastoma status and achieved without significant attenuation of androgen signaling (26). Herein, we described the evaluation of two new CDK4/6 inhibitors, G1T28 and G1T38, and demonstrated that both of these drugs have significant efficacy in animal models of CRPC. Notably, G1T28 and G1T38 effectively inhibited the growth of prostate cancer cells expressing wild-type AR (VCaP), AR-V7 (22Rv1 and LNCaP), and those expressing the AR F876L mutant. Similar to palbociclib, the antiproliferative activities of these compounds were not influenced by AR status and only manifested in retinoblastoma-expressing cells. Importantly, their efficacy was greater than the standard-of-care comparator enzalutamide and similar to docetaxel in all of the models in which they were studied. Currently, taxanes are the primary therapeutic option for patients whose tumors express AR-V7. The results of these studies suggest that CDK4/6i may have utility in this setting (29).

Despite demonstrated therapeutic efficacy palbociclib, ribociclib, and to a lesser extent abemaciclib, have been associated with clinically relevant myelosuppression in up to 65% of patients (19, 30). Although the neutropenia associated with CDK4/6i in most circumstances is manageable, it is likely to limit concomitant use of CDK4/6 inhibitors with other agents that suppress hematopoiesis. Although requiring a more comprehensive evaluation in humans, it is significant that in the mouse models used in this study, we observed significant accumulation of G1T28 and G1T38 within tumors, suggesting that it might be possible to achieve tumor suppression with these drugs at doses that do not result in significant myelosuppression. Thus, although myelosuppression is likely to be a class effect of CDK4/6 inhibitors, the properties of G1T28 and G1T38 may mitigate the impact of these drugs on the bone marrow permitting their use in continuous dosing regimens.

Palbociclib, although having modest efficacy when used as a single agent in breast cancer, has demonstrated considerable efficacy when used in combination with endocrine therapy. In patients with ER$^+$ breast cancers with cyclin D1 amplification (or p16 loss), for instance, a 2-fold increase in progression-free survival (PFS) was noted in those treated with the combination of palbociclib and letrozole (aromatase inhibitor) versus letrozole alone (18). A similar improvement in PFS (9.6 vs. 4.6 months) was noted in patients treated with

palbociclib plus fulvestrant versus fulvestrant alone (19). The benefit of combining CDK4/6 inhibitors with other agents is likely to extend to other retinoblastoma-positive tumors. In CRPC, the expression of the AR-V7 splice variant in circulating tumor cells is associated with resistance to enzalutamide and abiraterone (6). Although AR variant activity is reported to be dependent upon the full-length receptor, we and others have shown that the growth of tumors derived from these cells is not inhibited by competitive antagonists (31). It was significant, however, that we observed that G1T28 and G1T38 attenuated the growth of AR-V7–dependent/driven tumors when used as single agents. It will be of interest to see whether their use in combination with taxanes will result in improved therapeutic benefit, although it is unclear how their dramatic antiproliferative activity will impact taxane pharmacology.

Resistance to CDK4/6i is an emerging issue, and although retinoblastoma loss is a primary mechanism by which this can occur, there is substantial evidence demonstrating that resistance can occur regardless of retinoblastoma status or integrity (32). Combination therapy has also shown the potential to delay the development of resistance to palbociclib. In cellular models of ER^+ breast cancers, for instance, it has been observed that chronic palbociclib treatment leads to the outgrowth of a small population of cells exhibiting elevated cyclin E and CDK2 expression, thus bypassing the need for the cyclin D/CDK4/6 complex (32). Similar mechanisms of resistance to palbociclib have also been observed in cellular models of ovarian cancer (33). Such resistance can be circumvented somewhat by cotreatment of cells with palbociclib and a PI3K inhibitor, although this blockage can be bypassed by upregulation of the expression of cyclin E (32). Not surprisingly, given the interplay and preclinical success of dual inhibition of PI3K and CDK4/6, there are ongoing clinical trials assessing combined PI3K and CDK4/6 inhibitors in advanced ER^+ breast cancer patients (clinical trials #: NCT02684032 and NCT02088684). In our models of prostate cancer, however, we did not observe any benefit of combining a PI3K inhibitor with G1T38 *in vitro* (not shown). This result suggests that resistance to CDK4/6 inhibitors in prostate cancer may not occur in the same manner as observed in breast cancer and may be an area for future investigation.

The CDK4/6 inhibitors G1T28 and G1T38 exerted antiproliferative effects in relevant animal models of CRPC when used as single agents. Notably, the CDK4/6 inhibitors tested were as effective as taxanes in tumor models of enzalutamide-resistant disease with less toxicity (weight loss). In tumor models that were resistant to enzalutamide, the efficacy of CDK4/6 inhibitors was comparable with taxanes. When taken together, these data highlight the potential clinical utility of CDK4/6 inhibitors in prostate cancer and underscore the need for near-term clinical studies of these agents in patients with advanced prostate cancer.

Supplementary Material

Refer to Web version on PubMed Central for supplementary material.

Acknowledgments

Grant Support

This work was supported by a research grant from G1 Therapeutics (to D.P. McDonnell).

The costs of publication of this article were defrayed in part by the payment of page charges. This article must therefore be hereby marked *advertisement* in accordance with 18 U.S.C. Section 1734 solely to indicate this fact.

References

1. Siegel RL, Miller KD, Jemal A. Cancer statistics, 2015. CA Cancer J Clin 2015;65:5–29. [PubMed: 25559415]
2. Heinlein CA, Chang C. Androgen receptor in prostate cancer. Endocr Rev 2004;25:276–308. [PubMed: 15082523]
3. Wong YNS, Ferraldeschi R, Attard G, de Bono J. Evolution of androgen receptor targeted therapy for advanced prostate cancer. Nat Rev Clin Oncol 2014;11:365–76. [PubMed: 24840076]
4. Joseph JD, Lu N, Qian J, Sensintaffar J, Shao G, Brigham D, et al. Aclinically relevant androgen receptor mutation confers resistance to second-generation antiandrogens enzalutamide and ARN-509. Cancer Discov 2013;3: 1020–9. [PubMed: 23779130]
5. Balbas MD, Evans MJ, Hosfield DJ,Wongvipat J, Arora VK,Watson PA, et al. Overcoming mutation-based resistance to antiandrogens with rational drug design. Elife 2013;2:e00499. [PubMed: 23580326]
6. Antonarakis ES, Lu C, Wang H, Luber B, Nakazawa M, Roeser JC, et al. AR-V7 and resistance to enzalutamide and abiraterone in prostate cancer. N Engl J Med 2014;371:1028–38. [PubMed: 25184630]
7. Watson PA, Arora VK, Sawyers CL. Emerging mechanisms of resistance to androgen receptor inhibitors in prostate cancer. Nat Rev Cancer 2015;15: 701–11. [PubMed: 26563462]
8. Locke JA, Guns ES, Lubik AA, Adomat HH, Hendy SC, Wood CA, et al. Androgen levels increase by intratumoral de novo steroidogenesis during progression of castration-resistant prostate cancer. Cancer Res 2008;68: 6407–15. [PubMed: 18676866]
9. Taplin ME, Bubley GJ, Shuster TD, Frantz ME, Spooner AE, Ogata GK, et al. Mutation of the androgen-receptor gene in metastatic androgen-independent prostate cancer. N Engl J Med 1995;332:1393–8. [PubMed: 7723794]
10. Beer TM, Tombal B. Enzalutamide in metastatic prostate cancer before chemotherapy. N Engl J Med 2014;371:1755–6.
11. de Bono JS, Logothetis CJ, Molina A, Fizazi K, North S, Chu L, et al. Abiraterone and increased survival in metastatic prostate cancer. N Engl J Med 2011;364:1995–2005. [PubMed: 21612468]
12. Kroon J, Kooijman S, Cho NJ, Storm G, van der Pluijm G. Improving taxane-based chemotherapy in castration-resistant prostate cancer. Trends Pharmacol Sci 2016;37:451–62. [PubMed: 27068431]
13. Petrylak DP, Tangen CM, Hussain MH, Lara PN, Jr, Jones JA, Taplin ME, et al. Docetaxel and estramustine compared with mitoxantrone and prednisone for advanced refractory prostate cancer. N Engl J Med 2004; 351:1513–20. [PubMed: 15470214]
14. de Bono JS, Oudard S, Ozguroglu M, Hansen S, Machiels JP, Kocak I, et al. Prednisone plus cabazitaxel or mitoxantrone for metastatic castration-resistant prostate cancer progressing after docetaxel treatment: a randomised open-label trial. Lancet 2010;376:1147–54. [PubMed: 20888992]
15. Balk SP, Knudsen KE. AR, the cell cycle, and prostate cancer. Nucl Recept Signal 2008;6:e001. [PubMed: 18301781]
16. Vidula N, Rugo HS. Cyclin-dependent kinase 4/6 inhibitors for the treatment of breast cancer: a review of preclinical and clinical data. Clin Breast Cancer 2016;16:8–17. [PubMed: 26303211]
17. VanArsdale T, Boshoff C, Arndt KT, Abraham RT. Molecular pathways: targeting the cyclin D-CDK4/6 axis for cancer treatment. Clin Cancer Res 2015;21:2905–10. [PubMed: 25941111]
18. Finn RS, Crown JP, Lang I, Boer K, Bondarenko IM, Kulyk SO, et al. The cyclin-dependent kinase 4/6 inhibitor palbociclib in combination with letrozole versus letrozole alone as first-line treatment of oestrogen receptor-positive, HER2-negative, advanced breast cancer (PALOMA-1/TRIO-18): a randomised phase 2 study. Lancet Oncol 2015;16:25–35. [PubMed: 25524798]
19. Cristofanilli M, Turner NC, Bondarenko I, Ro J, Im SA, Masuda N, et al. Fulvestrant plus palbociclib versus fulvestrant plus placebo fortreatment of hormone-receptor-positive, HER2-

negative metastatic breast cancer that progressed on previous endocrine therapy (PALOMA-3): final analysis of the multicentre, double-blind, phase 3 randomised controlled trial. Lancet Oncol 2016;17:425–39. [PubMed: 26947331]

20. Finn RS, Aleshin A, Slamon DJ. Targeting the cyclin-dependent kinases (CDK) 4/6 in estrogen receptor-positive breast cancers. Breast Cancer Res 2016;18:17. [PubMed: 26857361]
21. Infante J, Shapiro G, Witteveen P, Gerecitano J, Ribrag V, Chugh R, et al. A phase I study of the single-agent CDK 4/6 inhibitor LEE011 in pts with advanced solid tumors and lymphomas. J Clin Oncol 2014;32:2528.
22. Flaherty KT, LoRusso PM, DeMichele A, Abramson VG, Courtney R, Randolph SS, et al. Phase I, dose-escalation trial of the oral cyclin-dependent kinase 4/6 Inhibitor PD 0332991, administered using a 21-day schedule in patients with advanced cancer. Am Assoc Cancer Res 2012;18: 568–76.
23. Patnaik A, Rosen LS, Tolaney SM, Tolcher AW, Goldman JW, Gandhi L, et al. Efficacy and safety of abemaciclib, an inhibitor of CDK4 and CDK6, for patients with breast cancer, non–small cell lung cancer, and other solid tumors. Cancer Discov 2016;6:740–53. [PubMed: 27217383]
24. Bisi JE, Sorrentino JA, Roberts PJ, Tavares FX, Strum JC. Preclinical characterization of G1T28: a novel CDK4/6 inhibitor for reduction of chemotherapy-induced myelosuppression. Mol Cancer Ther 2016;15:783–93. [PubMed: 26826116]
25. Sorrentino J, Bisi J, Roberts P, Strum J. G1T38, a novel, oral, potent and selective CDK 4/6 inhibitor for the treatment of Rb competent tumors [abstract]. In: Proceedings of the 107th Annual Meeting of the American Association for Cancer Research; 2016 4 16–20; New Orleans, LA. Philadelphia, PA: AACR; 2016. Abstract nr 2824.
26. Comstock CE, Augello MA, Goodwin JF, de Leeuw R, Schiewer MJ, Ostrander WF, Jr, et al. Targeting cell cycle and hormone receptor pathways in cancer. Oncogene 2013;32:5481–91. [PubMed: 23708653]
27. Ohtani K, DeGregori J, Nevins JR. Regulation of the cyclin E gene by transcription factor E2F1. Proc Natl Acad Sci U S A 1995;92:12146–50. [PubMed: 8618861]
28. Korpal M, Korn JM, Gao X, Rakiec DP, Ruddy DA, Doshi S, et al. An F876L mutation in androgen receptor confers genetic and phenotypic resistance to MDV3100 (enzalutamide). Cancer Discov 2013;3:1030–43. [PubMed: 23842682]
29. Antonarakis ES, Lu C, Luber B, Wang H, Chen Y, Nakazawa M, et al. Androgen receptor splice variant 7 and efficacy oftaxane chemotherapy in patients with metastatic castration-resistant prostate cancer. JAMA Oncol 2015;1:582–91. [PubMed: 26181238]
30. O'Sullivan CC. Overcoming endocrine resistance in hormone-receptor positive advanced breast cancer-the emerging role of CDK4/6 inhibitors. Int J Cancer Clin Res 2015;2:pii:029. [PubMed: 26726315]
31. Xu D,Zhan Y, Qi Y,Cao B,Bai S,Xu W,et al. Androgen receptor splice variants dimerize to transactivate target genes. Cancer Res 2015;75:3663–71. [PubMed: 26060018]
32. Herrera-Abreu MT, Palafox M, Asghar U, Rivas MA, Cutts RJ, Garcia-Murillas I, et al. Early adaptation and acquired resistance to CDK4/6 inhibition in estrogen receptor-positive breast cancer. Cancer Res 2016; 76:2301–13. [PubMed: 27020857]
33. Taylor-Harding B, Aspuria PJ, Agadjanian H, Cheon DJ, Mizuno T, Greenberg D, et al. Cyclin E1 and RTK/RAS signaling drive CDK inhibitor resistance via activation of E2F and ETS. Oncotarget 2015;6:696–714. [PubMed: 25557169]

Implications: The preclinical efficacy of CDK4/6 monotherapy observed here suggests the need for near-term clinical studies of these agents in advanced prostate cancer.

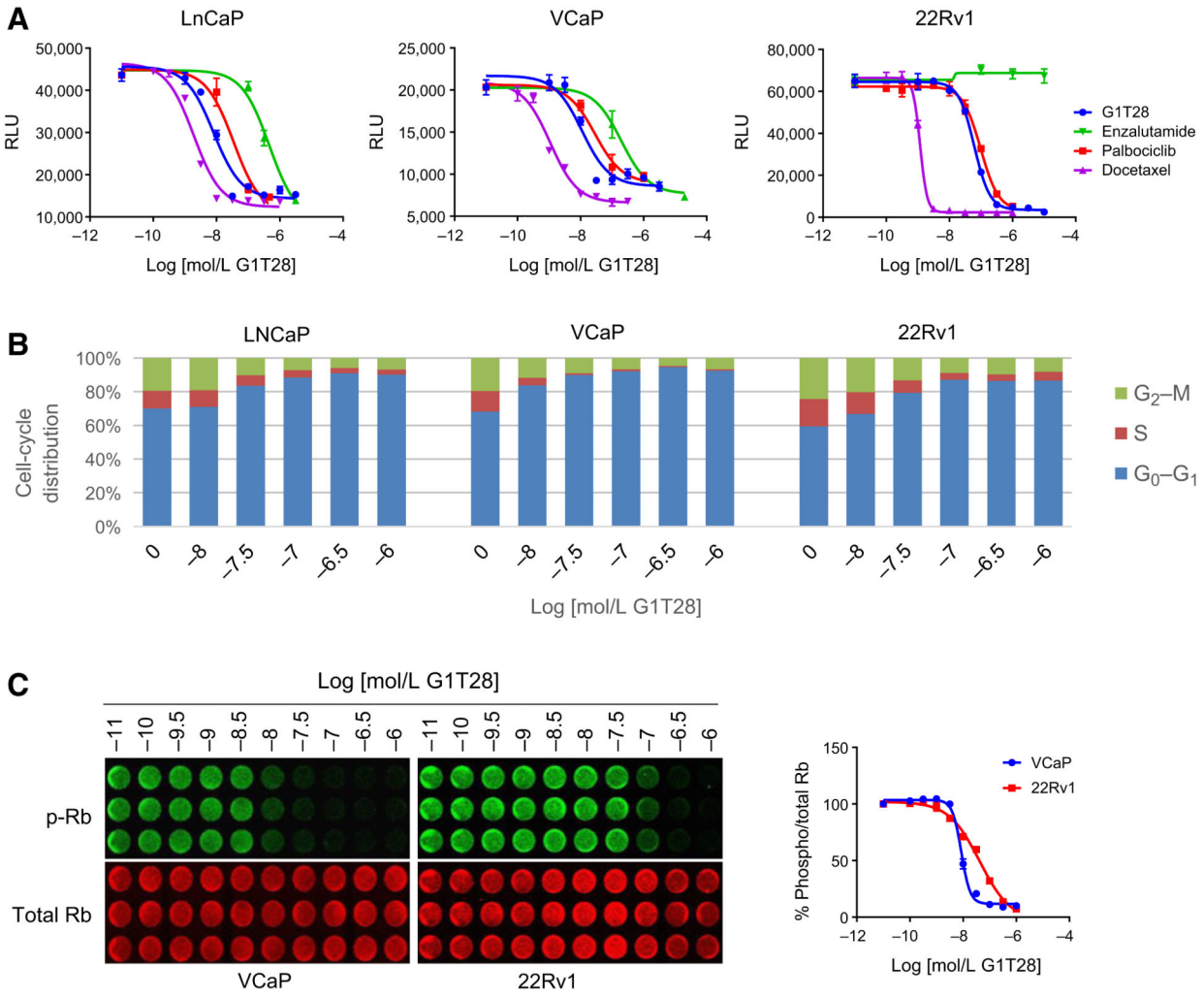

Figure 1.

G1T28 inhibits cell-cycle progression in models of prostate cancer. **A,** LNCaP, VCaP, or 22Rv1 cells were plated in media containing 10% FBS and treated with increasing concentrations of enzalutamide, docetaxel, palbociclib, or G1T28 (10^{-10}-$10^{-4.3}$ mol/L) and measured for cell viability by Hoechst staining after 5 to 7 days of treatment. **B** and **C,** LNCaP, VCaP, or 22Rv1 cells were plated in media containing 10% FBS with increasing concentrations of G1T28 ($10^{-9.5}$-10^{-6} mol/L) for 24 hours and then stained with PI for cell-cycle analysis (**B**) or fixed, permeabilized, and stained for phospho (Ser 807/811) and total Rb using a LI-COR Odyssey Clx imager (**C**). Dose–response curves were generated from densitometry of the phospho and total retinoblastoma expression using LI-COR Image Studio software. Data are representative of at least three independent experiments.

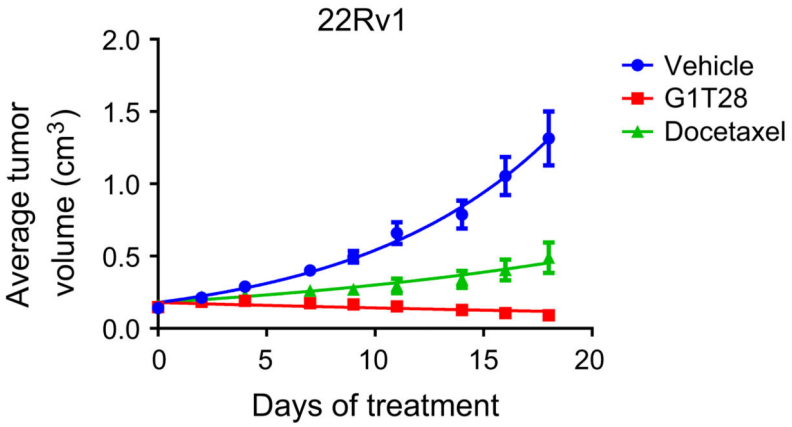

Figure 2.

G1T28 inhibits the growth of AR-V7^{+} xenograft prostate tumors. Castrated male nu/nu mice bearing 22Rv1 xenograft tumors were randomized (n = 17/group) to treatment with vehicle, G1T28 (100 mg/kg orally, daily) or docetaxel (20 mg/kg i.p., every week) when tumor volume reached approximately 0.1 cm^3. Average tumor volume ± SEM throughout treatment are presented.

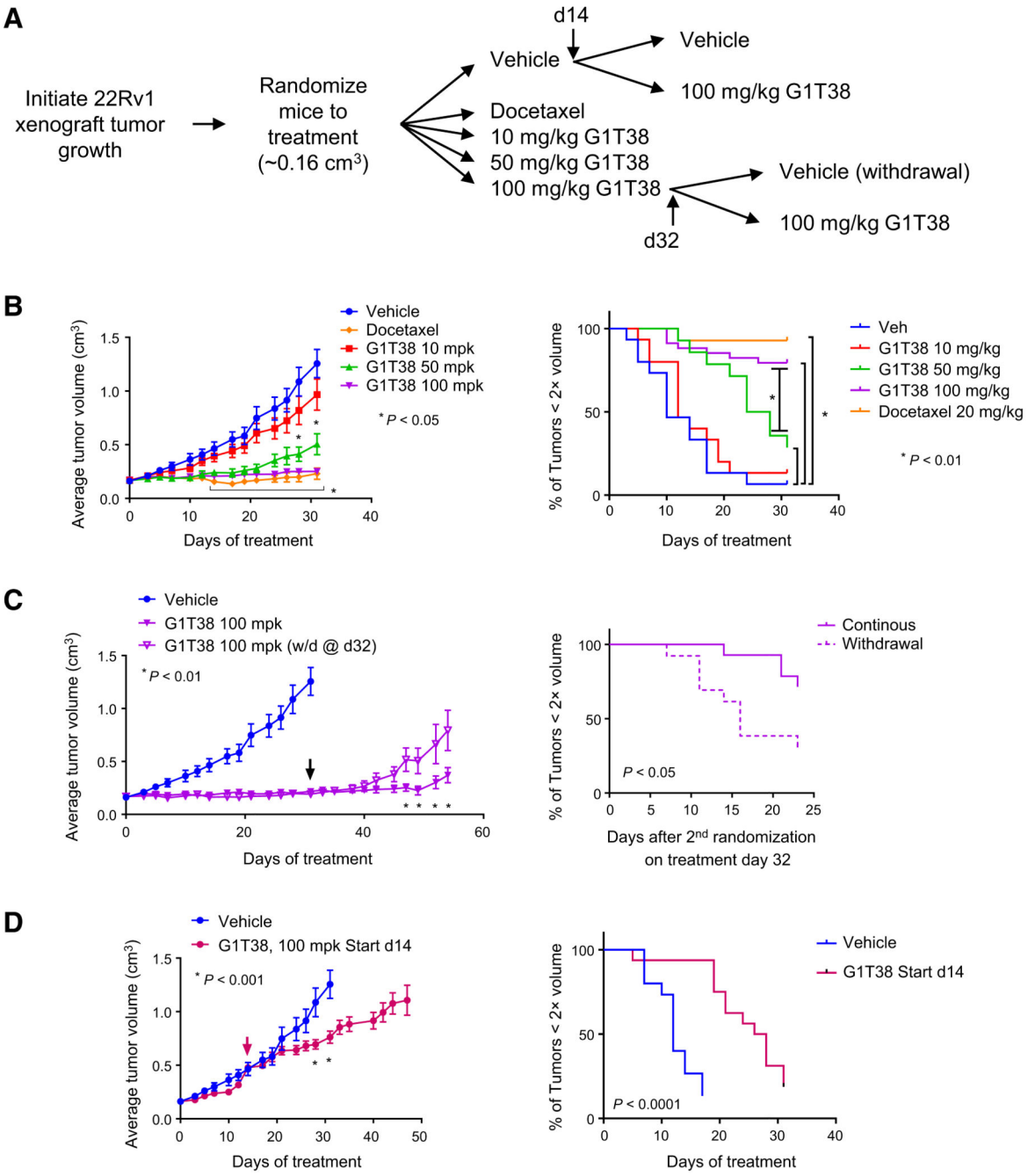

Figure 3.

Tumor growth suppression by CDK4/6i is dependent upon starting tumor volume and continuous exposure. **A,** Experimental outline: 22Rv1 xenograft tumors were initiated in castrated nu/nu mice and allowed to reach approximately 0.15 cm^3 volume prior to randomization treatment with vehicle ($n = 31$), with 20 mg/kg docetaxel (intraperitoneally, every week), or with 10, 50, or 100 mg/kg G1T38 (orally, every day, $n = 15$, 14, and 27, respectively). On treatment day 14, vehicle-treated animals were rerandomized to continue to receive vehicle ($n = 15$) or to treatment with G1T38 (100 mg/kg orally, every day, $n = 16$).

On treatment day 32, mice receiving 100 mg/kg G1T38 were rerandomized to continue to receive 100 mg/kg G1T38 ($n = 14$) or to treatment with vehicle ($n = 13$). Average tumor volume ± SEM of animals treated as described are presented in **B–D**, as well as time (days) required to reach 2× tumor volume as compared with initial volume on day 0. **B,** Average tumor volume ± SEM of all treatment groups during treatment days 0 to 31. Two-way ANOVA analysis followed by Bonferroni multiple comparison test determined that significant tumor growth inhibition ($P < 0.05$) was observed for 10 mg/kg G1T38 (days 28 and 31) and for 50 or 100 mg/kg G1T38 or docetaxel treatment (days 14–31). Standard Kaplan–Meier analysis of time to endpoint indicated a significant growth delay using an adjusted Bonferroni cutoff of $P < 0.01$. **C,** Averagetumor volume ± SEM of vehicle and 100 mg/kg G1T38 (continuous and withdrawal on treatment day 32). Two-way ANOVA analysis followed by Bonferroni multiple comparison test, as well as Kaplan–Meier analysis, determined that significant tumor growth ($P < 0.05$) was observed on treatment days 47 to 54 for animals rerandomized to vehicle after treatment day 31 (arrow). **D,** Average tumor volume ± SEM of vehicle and 100 mg/kg G1T38 (treatment days, 14–47). Two-way ANOVA analysis followed by Bonferroni multiple comparison test, as well as Kaplan–Meier analysis, determined that significant tumor growth inhibition ($P < 0.05$) was observed following rerandomization to treatment with 100 mg/kg G1T38.

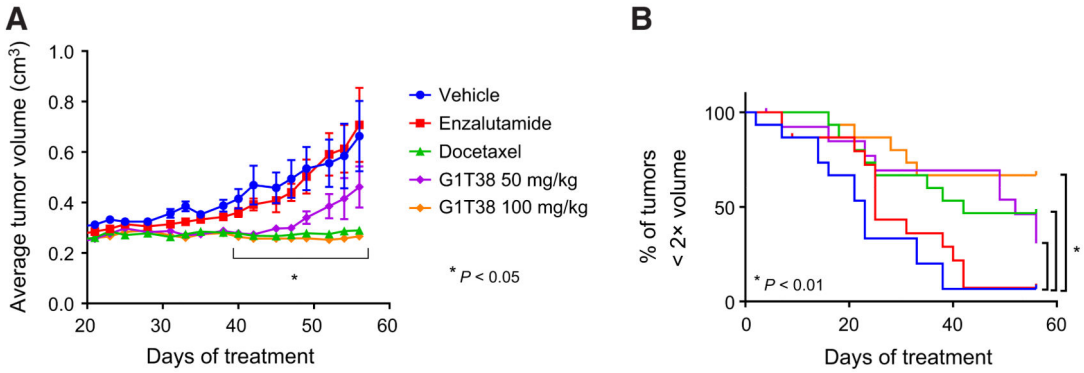

Figure 4.

G1T38 inhibits the growth of AR F876L^{+} xenograft tumors. Castrated male NSG mice bearing LNCaP-AR-F876L xenograft tumors were randomized to 8 weeks of treatment with vehicle, Enzalutamide (30 mg/kg orally, every day), G1T38 (50 or 100 mg/kg orally, every day), or docetaxel (20 mg/kg i.p., every week). Both time-to-progression analysis (with an adjusted Bonferroni cutoff of $P < 0.01$; **B**) and two-way ANOVA comparison of average tumor volumes throughout treatment (**A**), followed by Bonferroni multiple comparison test, indicated significant tumor growth inhibition by G1T38 (50 and 100 mg/kg) and by docetaxel on treatment days 40 to 56.

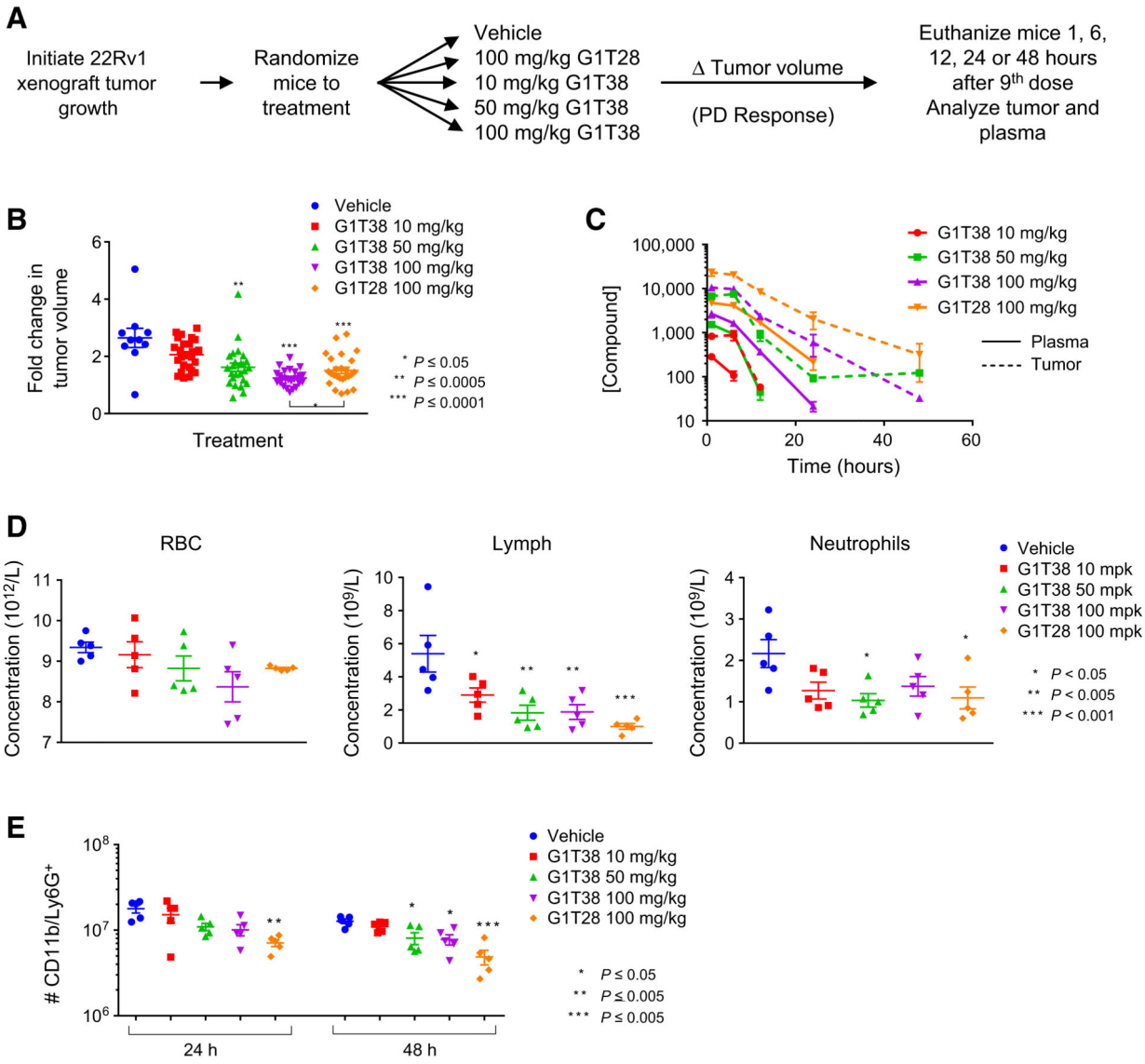

Figure 5.

G1T28 and G1T38 exhibit longer half-life in tumors than in plasma. **A,** Experimental outline: 22Rv1 xenograft tumors were initiated in castrated male nu/nu mice 12 days prior to the animals being randomized (average tumor volume per group = 0.19 cm^3) to treatment with vehicle, G1T28 (100 mg/kg), or G1T38 (10, 50, or 100 mg/kg) orally, every day. Mice were euthanized 1, 6, 12, 24, or 48 hours after the 9th dose (treatment day 8). **B,** Fold change in tumor volume (with mean and SEM indicated) after 7 days of treatment. ANOVA analysis followed by Bonferroni multiple comparison indicated significant repression of tumor by G1T28 and G1T38 (50 and 100 mg/kg). At equivalent doses (100 mg/kg), G1T38 induced greater tumor growth suppression than did G1T28. **C,** Drug levels of G1T28 and G1T38 present in tumor tissues (dashed lines) and in plasma (solid lines) 1, 6, 12, 24, or 48 hours after final dose were analyzed by LC/MS-MS. **D,** ANOVA analysis, followed by Bonferroni multiple comparison test, of CBC counts conducted on whole blood taken from animals euthanized 1 hour after final dose (after 9 days of treatment) revealed no change in red blood

cell density (left), reduced levels of lymphocytes (middle), and significant reduction of neutrophil numbers only in animals receiving 50 mg/kg G1T38 and 100 mg/kg G1T28. **E,** Bone marrow isolated from animals euthanized 24 or 48 hours after the final treatment in the above pharmacokinetic/pharmacodynamic analysis was analyzed by immunostaining (CD11b and $Ly6G^+$) and flow cytometry. Reduced bone marrow neutrophil number (as determined by ANOVA analysis and Bonferroni multiple comparison test) was observed in animals receiving 50 or 100 mg/kg G1T38 or G1T28 ($P < 0.05$).